Journal of Molecular Liquids 301 (2020) 112456

Contents lists available at ScienceDirect

Journal of Molecular Liquids

journal homepage: www.elsevier.com/locate/molliq

Adsorption characteristics of anionic surfactant onto laterite soil with differently charged surfaces and application for cationic dye removal

Tien Duc Pham [a,*], Thu Thao Pham [a], Minh Nguyet Phan [a], Thi Mai Viet Ngo [b], Van Doan Dang [c], Cuong Manh Vu [d,e,**]

[a] VNU University of Science, Vietnam National University, Hanoi, 19 Le Thanh Tong, Hoan Kiem, Hanoi 100000, Vietnam
[b] Thai Nguyen University of Education, Thai Nguyen University, 20 Luong Ngoc Quyen, Quang Trung, Thai Nguyen, Viet Nam
[c] Institute of Forensic Science, Ministry of Public Security, 99 Nguyen Tuan, Thanh Xuan, Hanoi, Viet Nam
[d] Center for Advanced Chemistry, Institute of Research and Development, Duy Tan University, Da Nang, Viet Nam
[e] Chemical Department, Le Quy Don Technical University, 236 Hoang Quoc Viet, Hanoi, Viet Nam

ARTICLE INFO

Article history:
Received 29 October 2019
Received in revised form 26 December 2019
Accepted 2 January 2020
Available online 7 January 2020

Keywords:
Surfactant adsorption
Laterite soil
Zeta potential
Rhodamine B
Two-step model

ABSTRACT

In this paper, we report the adsorption characteristics of the anionic surfactant, sodium dodecyl sulfate (SDS) onto laterite soil with positively and negatively charged surfaces. The laterite soil was characterized using X-ray fluorescence (XRF), scanning electron microscopy (SEM), as well as total organic carbon (TOC), Brunauer-Emmett-Teller (BET) and zeta potential measurements. The adsorption of SDS onto a positively charged laterite surface at pH 4 decreased with an increase in ionic strength, indicating that the electrostatic attraction was the main driving force for controlling the adsorption. On the other hand, the adsorption of SDS onto a negatively charged laterite surface at pH 10 was induced by both electrostatic and hydrophobic interactions as the adsorption increased with increasing NaCl concentrations. The adsorption isotherms of SDS onto laterite at different pH values and NaCl concentrations were fitted well by the two-step adsorption model. The adsorption mechanism of SDS onto laterite soil with differently charged surfaces was discussed in detail based on the changes in functional surface groups determined by Fourier transform infrared spectroscopy (FT-IR), variation in the change in surface charge as evaluated by zeta potential measurements, and adsorption isotherms. The application of SDS adsorption to the modification of the laterite surface for the removal of the cationic dye, rhodamine B (RhB) was also investigated. Optimum conditions for RhB removal were found to be pH 4, adsorption time 60 min, and adsorbent mass 0.25 g. The removal efficiency of RhB was >94% after five recycles. Our results indicate that the surface modification of laterite soil with SDS is valuable for the removal of cationic dyes from aqueous solutions.

1. Introduction

Ionic surfactants are extremely versatile amphoteric organic substances containing both hydrophilic head groups and hydrophobic hydrocarbon chains, which can easily dissolve in both organic solvents and aqueous media [1]. In the context of environmental remediation, ionic surfactants can be used for the removal of various contaminants from polluted soils and aquifer sediments [2]. In the presence of such surfactants, the solubilization of organic pollutants remained on the soil or sediment surfaces [3]. Ionic surfactants were also employed to modify many solid surfaces in order to enhance the removal efficiencies of various types of pollutants [4–9]. Therefore, numerous studies were conducted to determine the adsorption characteristics of ionic surfactant onto soil and mineral surfaces to predict the mechanism of pollutant remediation [10,11]. Ionic surfactant modified solid adsorbents and soils for pollutant removal were also investigated [9,12–18].

Laterite is a common soil present in tropical countries such as Vietnam. The characterization of Vietnamese laterite soil and adsorption of heavy metal ion onto laterite were previously studied [19]. Since laterite soil contains many metal oxides and natural organic matters (NOMs) [20], its charging behavior is strongly dependent on the solution pH. The adsorption of ionic surfactants onto laterite soil is rather complicated due to the charge regulation in the concomitant presence of proton [11,21]. Laterite soil has both positive and negative charges depending on the pH of the solution, while the charging properties of strong anionic surfactants are independent of pH. However, the adsorption of strong anionic surfactant onto laterites with differently charged surfaces has not been studied to date.

* Corresponding author: T.D. Pham, Faculty of Chemistry, VNU - University of Science, Vietnam National University - Hanoi
** Correspondence to: C.M. Vu, Center for Advanced Chemistry, Institute of Research and Development, Duy Tan University, Da Nang, Viet Nam.
E-mail addresses: tienduchphn@gmail.com, tienducpham@hus.edu.vn (T.D. Pham), vumanhcuong@duytan.edu.vn, vumanhcuong309@gmail.com (C.M. Vu).

https://doi.org/10.1016/j.molliq.2020.112456
0167-7322/

Organic dyes, which are typically released in developing countries from various industrial processes related to paints, cosmetic pigments, textiles, paper, food, etc., are serious pollutants in water environments. Many techniques have been developed for organic dye removal, such as photocatalytic degradation [22,23], advanced oxidation [24,25], coagulation/flocculation [26], and adsorption [27–30]. Among these, adsorption is one of the most suitable methods for use in developing countries as it relies on low cost adsorbents [31,32]. In particular, surfactant modified laterite soil is known to be a cheap adsorbent for organic dye removal. Nevertheless, a systematic study of the application of anionic surfactant adsorption for removal of organic dye has not been carried out so far.

To understand the characteristics of surfactant adsorption, it is important to develop a model based on the envisaged concept. A two-step adsorption theoretical model [33,34] was proposed focusing on the hemimicelle concept [34], from which a general adsorption isotherm equation was derived. Such two-step adsorption model was successfully applied to many types of surfactant adsorption isotherms as well as a number of systems related to the surfactant adsorption onto solid surfaces [8,11,19,30,34–37]. Thus, such model is suitable for surfactant adsorption onto both positively and negatively charged laterite surfaces.

In this work, we investigated for the first time the adsorption of a strong anionic surfactant, sodium dodecyl sulfate (SDS), onto laterite soil with differently charged surfaces. The two-step adsorption model was applied to fit the adsorption isotherms of SDS onto laterite soil at different values of pH and ionic strength. An adsorption mechanism was suggested based on the adsorption isotherms, surface modification by Fourier transform infrared spectroscopy (FT-IR) and change in the surface charge against SDS concentrations by zeta potential measurements. The application of the SDS adsorption to modified laterite surfaces for the removal of cationic dye, rhodamine B (RhB) was also investigated. The conditions for achieving an effective RhB removal using SDS modified laterite soil including contact time, pH, adsorbent dosage, and reuse potential of the adsorbent were experimentally determined.

2. Experimental

2.1. Materials and chemicals

The laterite soil was collected at Thach That, Hanoi, Vietnam. It was then pre-treated according to our previously reported protocol [19].

Sodium dodecyl sulfate (SDS) of special grade (purity > 95.0%), was supplied by Scharlau (Spain), and used in the present study without further purification. The cationic dye, methylene blue (MTB, with a purity higher than 98.5%) and organic solvent chloroform ($CHCl_3$, HPLC grade) were acquired from Scharlau (Spain) and used to determine the concentration of SDS by a spectrophotometric method. Rhodamine B, for microscopy (purity > 95.0%) with a molecular weight of 479.02 g/mol was obtained from Merck. Other chemicals (NaCl, HCl, and NaOH) were purchased from Merck (Germany) and were of analytical reagent grade. The solution pH was measured by a pH meter (HI 2215, Hanna, USA). The glass pH electrode was calibrated everyday with three standard buffers at pH 4.01, 7.01, and 10.01 (Hanna). Ultrapure water was produced by an ultrapure water system (Labconco, USA) with a resistivity of 18.2 MΩ·cm.

2.2. Characterization and analytical methods

The laterite soil was previously characterized using X-ray diffraction (XRD), Fourier transform infrared spectroscopy (FT-IR), and inductively coupled plasma mass spectrometry (ICP-MS) [19]. Herein, it was further characterized by X-ray fluorescence (XRF) spectroscopy, scanning electron microscopy (SEM), as well as total organic carbon (TOC), Brunauer-Emmett-Teller (BET), and zeta potential measurements.

The composition and impurities of laterite were examined using a fluorescent X-ray spectrometry (JSX-1000S, JEOL) in the presence of a Si semiconductor detector. A voltage from 5 to 30 kV with a step of 5 kV was applied. A total carbon analyzer TOC-V_{CPH} (Shimadzu, Japan) was used to determine the organic carbon in the laterite soil.

The SEM images were obtained with a Hitachi (H4800, Japan) and NIHE camera (7.9 mm ×100,000). The operating conditions were an accelerating condition of 10 kV and scale of 500 nm.

The adsorption and desorption isotherms of N_2 to calculate the specific surface area according to the BET method was measured with a TriStar 3000 (Micromeritics, USA). The adsorption isotherm of N_2 onto laterite was recorded at 77.35 K, equilibrium interval of 10 s and sample mass of 1.2585 g.

The zeta (ζ) potential was measured using a Zetasizer Nano ZS (Malvern) at room temperature of 25 ± 2 °C. The ζ potential was calculated from the electrophoretic mobility using the Smoluchowski equation (HS) [38]:

$$\zeta = \frac{u_e\,\eta}{\varepsilon_{rs}\,\varepsilon_0} \tag{1}$$

where ζ is the zeta potential (mV), u_e is the electrophoretic mobility (μm s^{-1}/V cm^{-1}), η is the dynamic viscosity of the liquid (mPa.s), ε_{rs} is the relative permittivity constant of the electrolyte solution and ε_0 is the electric permittivity of vacuum (8.854×10^{-12} F/m).

Ultra violet–visible (UV–Vis) spectroscopy was used to quantify the concentrations of SDS and RhB in the solutions.

The concentration of SDS was determined using a spectrophotometric method based on paired ion formation. The measurements of the samples as well as standard solutions or blanks were carried out simultaneously according to our previous report [11]. The absorbance of SDS-MTB in the chloroform phase was measured at a wavelength of 655 nm by using an UV–Vis spectrophotometer (UV-1650PC, Shimadzu).

The concentration of RhB was also determined by obtaining UV–Vis spectra at a wavelength of 554 nm. Under different experimental conditions, all blank and samples were simultaneously prepared and appropriately diluted. Subsequently, the concentration of RhB was quantified by using an UV–Vis spectrophotometer (UV-1650PC, Shimadzu) upon standard calibration. A correlation coefficient of calibration was achieved of at least 0.999.

FTIR analysis was performed with an affinity-1S spectrometer (Shimadzu, Japan). The FTIR spectra of the laterite soil before and after SDS adsorption at different pH values were recorded under the same conditions of atmospheric pressure, a temperature of 25 ± 2 °C and resolution of 4 cm^{-1}.

2.3. Adsorption study

The adsorption isotherms were conducted in 15 mL Falcon tubes at 25 ± 2 °C, controlled by an air conditioner.

For the SDS adsorption, 0.1 g of treated laterite was mixed with 10 mL of a NaCl solution at different concentrations by using an orbital shaker. Then, SDS concentrations ranging from 10^{-5} to 10^{-2} M were added, and the pH was adjusted to the original value. After 2 h, the Falcon tubes containing laterite and SDS were centrifuged at 6000 rpm with a centrifuge (DSC-200A-1, DIGISYSTEM, Taiwan). After SDS adsorption under optimum conditions, the surfactant modified laterite (SML) was formed.

For the RhB adsorption, a series of adsorbent amounts of SML was mixed with 10 mL of 10^{-5} M RhB to optimize some parameters for efficiency (pH, contact time and adsorbent mass). In order to determine the adsorption isotherms, different RhB concentrations ranging from 10^{-6} to 10^{-3} M were added under the same conditions at 1, 10, and 100 mM NaCl. The adsorption isotherms were obtained under optimum adsorption conditions of pH, contact time and adsorbent mass. After

equilibrium, the SML particles and RhB solutions were also separated by centrifugation.

Each adsorption experiment was conducted at least in three replicates to obtain a good standard deviation. The adsorption capacities of SDS and RhB onto laterite and SML, respectively were determined according to the following equation:

$$\Gamma = \frac{C_i - C_e}{m} \times V \times M \times 1000 \quad (2)$$

where Γ is the adsorption capacity of SDS or RhB (mg/g), C_i is the initial concentration of SDS or RhB (M), C_e is the equilibrium concentration of SDS or RhB (M), V is the volume of solution (L), M molecular weight of SDS or RhB (g/mol), and m is the adsorbent mass (g).

The adsorptive removal (%) of RhB was calculated by Eq. (3).

$$\text{Removal}\ (\%) = \frac{C_i - C_f}{C_i} \times 100\% \quad (3)$$

where C_i and C_f are the initial and final concentrations of RhB (mol/L), respectively.

The adsorption isotherms of SDS onto laterite at different values of pH and ionic strength as well as those of adsorption isotherms of RhB onto SML in the presence of different NaCl concentrations were fitted by a general isotherm equation. The equation was derived from the hemimicelle concept of two adsorption steps, in which the surfactants molecules can exist at the solid-liquid interface [34].

The general isotherm equation is

$$\Gamma = \frac{\Gamma_\infty k_1 Ce\left(\frac{1}{n} + k_2 Ce^{n-1}\right)}{1 + k_1 Ce\left(1 + k_2 Ce^{n-1}\right)} \quad (4)$$

where Γ is the amount of adsorbed SDS or RhB, Γ_∞ is the maximum adsorption amount of SDS or RhB, k_1 and k_2 are the equilibrium constants for the first step and second step, respectively and n is the number of hemimicelle for the SDS adsorption or clusters for the RhB adsorption. The selected fitting parameters were described in previous reports [11,30].

The hemimicelle concentration (HMC) in the two-step model for the SDS adsorption can be determined by the following equation:

$$HMC = \left(\frac{n-1}{n+1}\right)^{\frac{n+1}{n}} (k_1 k_2)^{\frac{-1}{n}} \quad (5)$$

3. Results and discussion

3.1. Characterization of laterite soil

According to our previous work [19], X-ray diffraction analysis confirmed that laterite soil is made of crystal structures of quartz (SiO_2), hematite (Fe_2O_3) and goethite (FeO(OH)). The functional groups corresponding to the Si—O—Fe, Al—OH, and Fe—OH vibrations were determined by FT-IR spectroscopy. Herein, the components of laterite soil were further examined by XRF and TOC in comparison with previous ICP-MS data [19]. The morphology and specific surface area of laterite soil were investigated by SEM and BET, respectively, while the charging behavior of the laterite particles was evaluated on the basis of ζ potential measurements.

The XRF and TOC measurements were used to determine the composition of the laterite soil. The result shown in Table 1 indicates that the main elements were Fe, Si, and Al. The organic carbon content was quite high compared to that of natural soil. The composition of laterite used in the present study was in good agreement with that of other laterite soil [20,39].

Table 1
Percentage composition of laterite soil determined by XRF.

Element	mass%	mol%	*SD*
Al	7.226	12.592	1.42
Si	10.444	17.488	1.28
Fe	78.23	65.85	0.16
P	0.22	0.34	1.55
K	0.27	0.33	0.62
Ca	0.07	0.08	0.40
TOC	0.80	–	0.02
Other	2.74	2.52	–

The SEM image of raw laterite soil shown in Fig. 1 indicates that laterite possesses at rough shape. Nevertheless, laterite is not porous material, suggesting that it may not have such a high specific surface area.

From the adsorption-desorption isotherm of N_2 on laterite shown in Fig. 2, a specific surface area of 66.97 m^2/g was obtained. The specific surface area of laterite in our case was smaller than that of an alkali treated laterite soil [40], while being rather high for natural minerals. In addition, the nonporous structure of laterite was also confirmed by the BET method.

The ζ potential of the laterite soil shown in Fig. 3 confirmed that charging behavior of laterite was strongly dependent on the pH of the solution. The point of zero charge (PZC) which equals to the isoelectric point (IEP) without any specific adsorption was found to be about 6.5. This value is in good agreement with previous studies [20,39].

The above results indicate that raw laterite soil is a natural mineral containing many dominant metal oxides such as Fe_2O_3, Al_2O_3, and SiO_2 as well as a high content of natural organic substances. Although

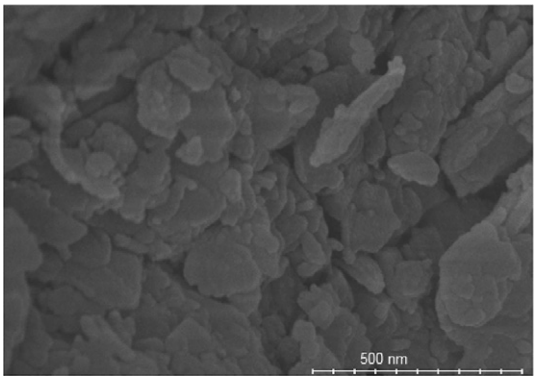

Fig. 1. The SEM image of raw laterite soil.

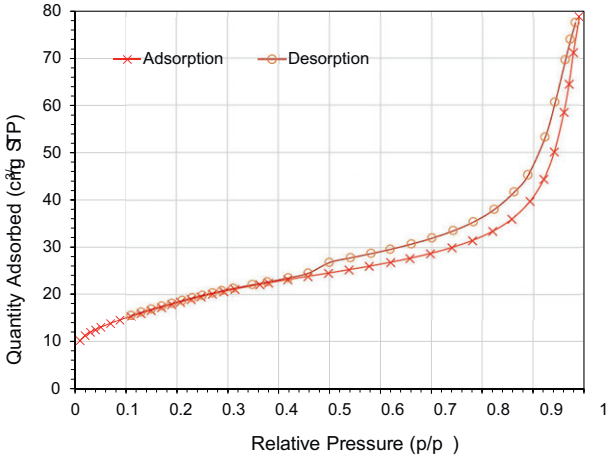

Fig. 2. Nitrogen adsorption-desorption isotherms on laterite soil.

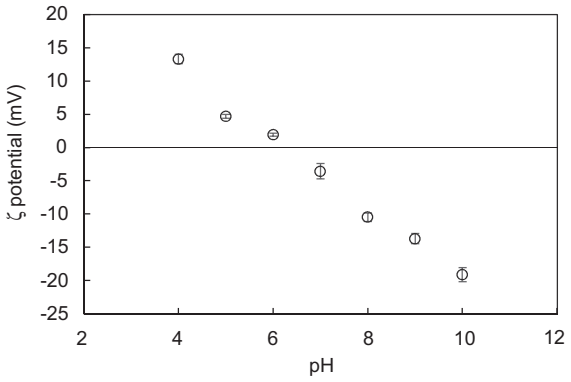

Fig. 3. The ζ potential of laterite soil as a function of pH at 1 mM NaCl.

laterite possesses a quite high specific surface area, the absolute charge density of this soil is not so high. To enhance the removal of the RhB dye, a surface modification is needed. To establish the modification conditions of the laterite surface, the adsorption of SDS onto laterite soil at pH 4 and 10 which corresponds to positive and negative charged laterite was systematically carried out as discussed below.

3.2. Adsorption of SDS onto laterite soil

3.2.1. Adsorption isotherms of SDS onto laterite soil with differently charged surfaces

The adsorption of SDS onto laterite soil at two salt concentrations with differently charged surfaces was well demonstrated by the isotherms. According to the above zeta potential measurements, laterite features positive and negative charges at pH 4 and pH 10, respectively. Since SDS is a strong anionic surfactant, its charging behavior and CMC are independent on the pH, however, the adsorption of SDS onto laterite soil at pH 4 and pH 10 has a different pattern.

At pH 4, the adsorption capacity of SDS onto laterite decreased with increasing NaCl concentration from 1 to 10 mM, mainly because the electrostatic attraction between the negatively charged DS- head groups and positively charged laterite surface is reduced with an increase in salt concentration. Although non-electrostatic interactions between the hydrocarbon chains of the surfactant molecules as well as natural organic matters (NOMs) in soils and hydrophobic groups in surfactants may play an important role for surfactant adsorption [10], the adsorption of SDS onto laterite in this case was mainly controlled by electrostatic interactions. At pH 10, the adsorption of SDS onto laterite increased with increasing NaCl concentrations from 1 to 10 mM, indicating that non-electrostatic interactions induced adsorption. Due to the high concentration of NOMs in the laterite soil, hydrophobic interactions between the alkyl chains of SDS and organic carbon in the soil was main driving force for adsorption. The adsorption of anionic surfactant onto differently charged surfaces is complicated due to charge adjustments [41]. In the present study, we investigated the adsorption of SDS onto laterite soil at two salt concentrations, i.e., 1 and 10 mM NaCl, since the critical micelle concentration (CMC) of SDS did not differ much. The CMC values were in fact 5.5 and 5.0 mM at 1 and 10 mM NaCl, respectively. On the other hand, when increasing the NaCl concentration to 50 mM, the CMC was 2.5 mM which make it difficult to evaluate the effect of the laterite surface charge at pH 4 and 10. Since a lower CMC influences the bilayer formation due to increase in hydrophobic interactions, the electrostatic attraction is hard to evaluate at low pH.

As it can be seen in Figs. 4 and 5, the solid lines fitted by the two-step adsorption model can reasonably represent the experimental data by using the fitting parameters shown in Table 2. From the fitting procedure, the n_{SDS} values of about 3.5 and 3.0 were chosen for the SDS adsorption at pH 4 and 10, respectively. Although the n_{SDS} values obtained from this model were smaller than the aggregation numbers

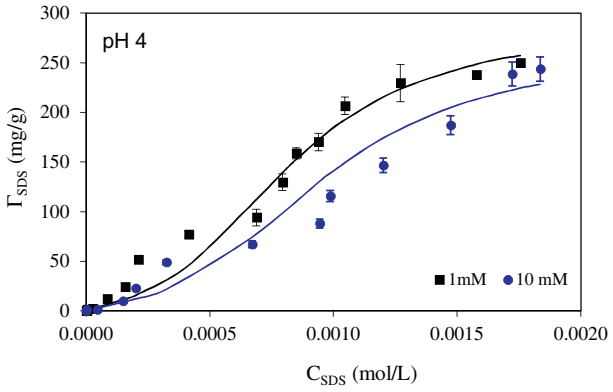

Fig. 4. Adsorption isotherms of SDS onto positively charged laterite surface at pH 4 in 1 mM and 10 mM NaCl. CSDS is the equilibrium SDS concentration. While the points are experimental data, the solid lines are the results of 2-step adsorption model. Error bars show the standard deviations of three replicates.

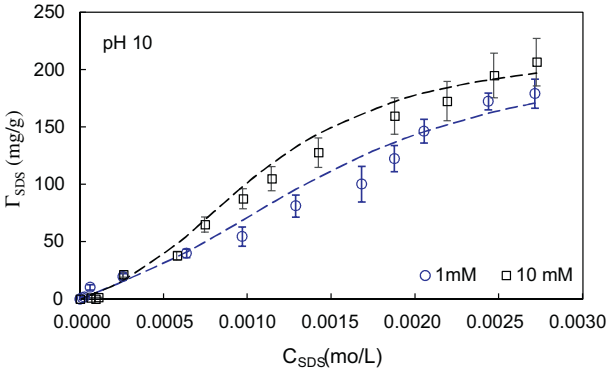

Fig. 5. Adsorption isotherms of SDS onto negatively charged laterite surface at pH 10 in 1 mM and 10 mM NaCl. CSDS is the equilibrium SDS concentration. While the points are experimental data, the dashed lines are the results of 2-step adsorption model. Error bars show the standard deviations of three replicates.

measured by experimental spectroscopic methods [42,43], the two-step model is useful to evaluate the effect of the ionic strength and the adsorption characteristics. It can be observed that the values of n_{SDS} and $k_{2,SDS}$ for the SDS adsorption onto positively charged laterite were higher than those for negatively charged laterite. The higher are the n_{SDS} and $k_{2,SDS}$ values, the steeper are the adsorption isotherms [34]. The values of $k_{2,SDS}$ at pH 4 were from 92 to 180 times greater than those at pH 10, Interestingly, at different pH and ionic strength, the values of $k_{2,SDS}$ did not change significantly, suggesting that hemimicelles were completely formed, while admicelles were more favored for surfactant adsorption onto oppositely charged surfaces than similar charge. The maximum adsorption capacity of SDS adsorption onto laterite soil with positive charges (pH 4) was also higher than that of anionic surfactant adsorption onto a negatively charged laterite surface (pH 10). The hemimicelles concentration (HMC) increased from 3.48×10^{-4} to 4.15×10^{-4} mol/L when increasing the ionic strength at pH 4, while the HMC decreased about 1.3 times upon

Table 2
Fitting parameters for the SDS adsorption onto laterite soil at different pH and ionic strength.

pH	C_{NaCl} (mM)	Γ_{SDS} (mg/g)	$k_{1,SDS}$ (g/mg)	$k_{2,SDS}$ $(g/mg)^{n-1}$	n_{SDS}	*HMC* (mol/L)
4.0	1	285	1×10^3	9×10^7	3.5	3.48×10^{-4}
	10	260	9×10^2	1.2×10^8	3.6	4.15×10^{-4}
10.0	1	215	1×10^3	5×10^5	3.0	5.00×10^{-4}
	10	220	9×10^2	1.3×10^6	3.0	3.87×10^{-4}

decreasing ionic strength from 10 to 1 mM NaCl at pH 10. This suggests that the HMC can be a parameter to evaluate the adsorption of SDS onto differently charged laterite surfaces.

To postulate an adsorption mechanism of SDS onto laterite soil with differently charged surfaces, it is necessary to determine the change in surface charge upon SDS adsorption by the variation in ζ potential as well as the differences in surface functional groups by FT-IR.

3.2.2. Adsorption mechanism of SDS onto laterite with differently charged surfaces

Herein, adsorption mechanisms of SDS onto laterite soil are discussed in detail based on the change in surfaces and functional groups by ζ potential measurements and FT-IR, respectively.

The measurement of the eta (ζ) potential is a useful method to evaluate the changes in the charging properties of different adsorption systems [44,45]. Although the ζ potential can be calculated by employing many techniques, electrophoretic mobility is the most widely used to study the change in surface charge of an adsorbent after adsorption. Figs. 6 and 7 show the ζ potential of laterite in the presence of different SDS concentrations in 1 and 10 mM NaCl at pH 4 and 10, respectively.

Fig. 6 shows that the ζ potential decreased with increasing SDS concentrations, then reached a constant value. At pH 4, the laterite soil was positively charged as confirmed by a ζ potential of 13.3 mV. Nevertheless, a charge reversal occurred when the SDS concentration was about 4 mM at both 1 and 10 mM NaCl background electrolyte. This concentration was close to CMC of SDS at the same NaCl concentration [46]. The high salt concentration and the low absolute values of the ζ potential, indicated that electrostatic attraction between the DS^- anion and oppositely charged laterite surface was important for adsorption.

On the other hand, the laterite soil was negatively charged at pH 10, therefore the charge reversal could not occur. Moreover, the adsorption of the DS^- anion onto the same negatively charged laterite required the higher concentrations of SDS (about 6 mM) to achieve the plateau charge. Interestingly, the absolute value of the ζ potential at 10 mM NaCl was higher than that at lower salt concentration [47]. This suggests that the electrostatic repulsion between the DS^- anion and negatively charged NOMs in laterite induced the adsorption. In other words, the adsorption of SDS onto negatively laterite surfaces is controlled by both electrostatic and non-electrostatic interactions.

The adsorption mechanism of SDS laterite soil with differently charged surfaces is deduced from FTIR spectra of the laterite soil before and after SDS adsorption at pH 4 and 10. Fig. 8 shows that the peaks at 2920 and 2856 cm^{-1} assigned to asymmetrical and symmetrical stretching vibrations of alkyl groups —CH_2—, respectively disappeared after adsorption at pH 4 while decreasing dramatically in the spectra at pH 10 compared to the case of the SDS powder (data not shown). These results suggested that that the hydrophobic interaction occurred onto the surface of laterite soil at pH 10, in analogy with the SDS adsorption onto α-Al_2O_3 surface [8]. On the other hand, the hydrophobic interaction was negligible for SDS adsorption onto the laterite soil at pH 4. Furthermore, peaks at 1247 and 1218 cm^{-1} characteristics of the SO_4^{2-} vibration disappeared in the spectra of the laterite soil after SDS adsorption at both pH 4 and 10. These results indicated that the electrostatic interaction contributed to the SDS adsorption onto the laterite soil. This is in good agreement with the ζ potential measurements. By taking into consideration the contribution of both hydrophobic and electrostatic interactions, Fig. 9 shows a cartoon of the SDS adsorption on laterite soil in which admicelles with a SDS bilayer containing both a first layer head-on toward the laterite soil with positively charged surface and second layer head- out toward the solution were formed at pH 4 while the reverse micelle formation occurred on the laterite surface

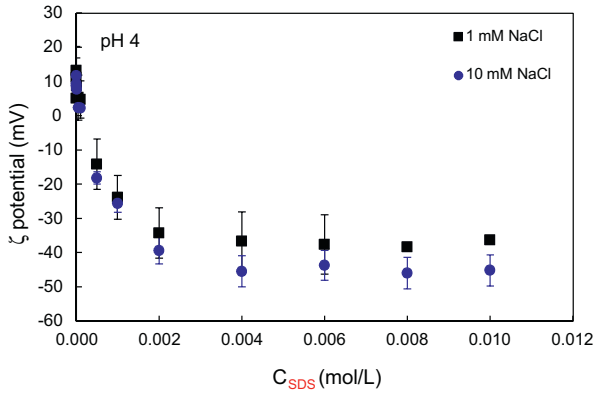

Fig. 6. The ζ potential of laterite as the function of initial SDS concentration at pH 4 in 1 mM and 10 mM NaCl.

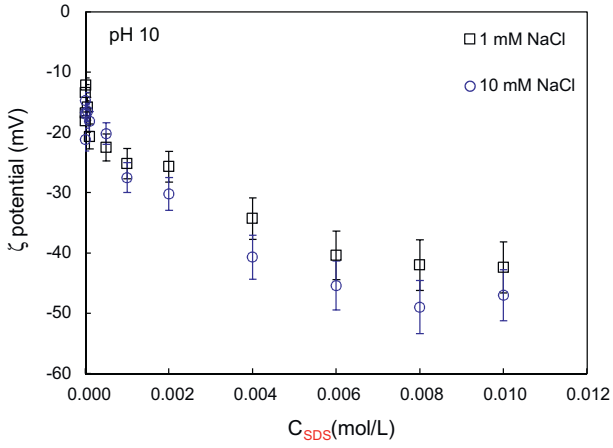

Fig. 7. The ζ potential of laterite as the function of initial SDS concentration at pH 10 in 1 mM and 10 mM NaCl.

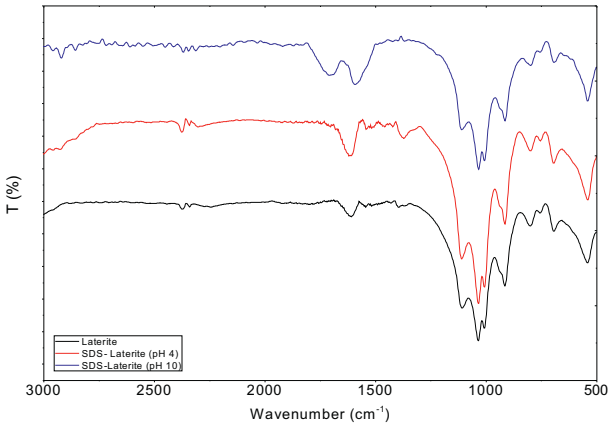

Fig. 8. FT-IR spectra of laterite, laterite after SDS adsorption at pH 4 and laterite after SDS adsorption at pH 10.

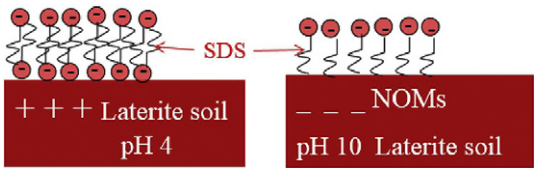

Fig. 9. The cartoon representation of SDS adsorption onto positively charged laterite soil surface at pH 4 and negative charge of laterite in the presence of natural organic matters (NOMs) at pH 10.

with a negative charge due to NOMs at pH 10. These results are similar to those described for the SDS adsorption onto a Au-CaF_2 film coated with amine groups [48].

The adsorption of SDS onto laterite soil with at two different pH and salt concentration values corresponds to the equilibrium state. The adsorption of a surfactant onto the soil is complicated due to the compositions of the real soil which contains many metal oxides and NOMs. The dynamic adsorption of SDS onto laterite soil maybe environmentally important. Nevertheless, for the application of SDS surface –modified laterite soil to removal of cationic dyes, an equilibrium study is necessary.

The above results imply that to achieve a higher adsorption capacity during the SDS adsorption onto positively charged laterite surfaces with admicelles formation is much better for modification of the laterite surface. The laterite soil with an SDS modification can be employed for removal of many cationic dyes due to its highly negative charge. Table 3 shows that high adsorption capacities and removal efficiencies of cationic dyes such as crystal violet, methylene blue and RhB were obtained when using a surfactant-modified laterite. Since, RhB is highly toxic and more stable than two other cationic dyes, we only investigated the systematic removal of RhB using the surfactant-modified laterite.

To enhance the removal of RhB, the SDS adsorption onto laterite at pH 4 and 1 mM NaCl was used for further studies as described below.

3.3. Adsorptive removal of rhodamine B using SDS modified laterite (SML)

3.3.1. Effect of pH

The solution pH is an important factor for RhB adsorption since it strongly influences to the surface charge and charging properties of RhB. The influence of pH on the RhB removal at an initial RhB concentration of 10^{-5} M using SML was investigated from pH 3 to 10 with a contact time of 60 min, adsorbent mass of 0.25 g, and 1 mM NaCl (Fig. 10).

Fig. 10 shows that the RhB removal using SML decreased from 94.9% to 57.0% when the pH increased from 4 to 10. Since RhB is cationic dye with positive charges within the 4–10 pH range, the RhB adsorption only depends on the surface charge of SML. The desorption of SDS can be induced by increasing the pH, therefore the adsorption of RhB decreased with increasing of the solution pH [9]. This can be explained by the SDS desorption that leads to a less negatively charged SML surface. Since the electrostatic attraction between positive RhB and negative SML is attenuated, the RhB adsorption decreases. The optimum pH was found to be 4 since the removal was maximal and the standard deviations of three replicates were minimal at pH 4.

Table 3
Adsorption capacity and removal efficiency of some cationic dyes using surfactant-modified laterite (SML).

Cationic dyes	Adsorption capacity (mg/g)	Removal efficiency (%)
Crystal violet	62.5	86.5
Methylene blue	15.5	83.5
Rhodamine B	18.0	98.85

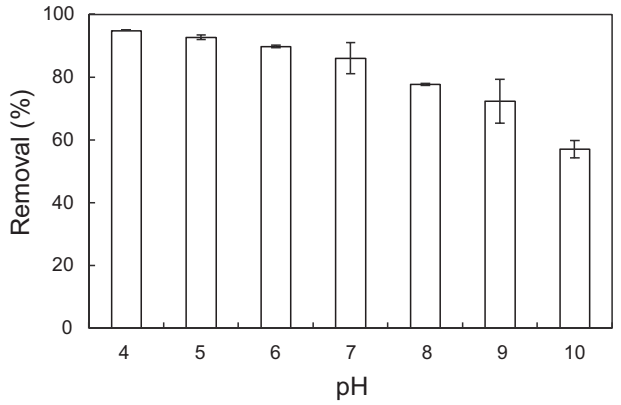

Fig. 10. Effect of pH on the removal of RhB by surfactant-modified laterite (SML) (initial concentration Ci (RhB) = 10–5 M, adsorbent mass 0.25 g, contact time 60 min, and 1 mM NaCl). Error bars show the standard deviations of three replicates.

3.3.2. Effect of contact time

The contact time influences the equilibrium adsorption and adsorption kinetics. The effect of the contact time on the RhB removal using SML from 5 to 240 min is shown in Fig. 11. It can be seen that the adsorption takes place very fast and it does not change significantly after 60 min. The contact time of RhB adsorption onto SML was much faster than that of the RhB adsorption on activated carbon (120 min) [49]. It also reached the equilibrium much more quickly than the RhB adsorption on synthesized nano γ-Al_2O_3 (180 min) [5]. Therefore, a contact time of 60 min was chosen to further investigate the RhB removal using SML.

3.3.3. Effect of adsorbent amount

The specific surface area represents an important factor that affects every adsorption system. The specific surface area of laterite was found to be 66.97 m^2/g (Section 3.1). Since it is influenced by a adsorbent amount, a study of adsorbent amount effect of the effect of the SML amounts on the RhB removal were carried out and the results are shown in Fig. 12.

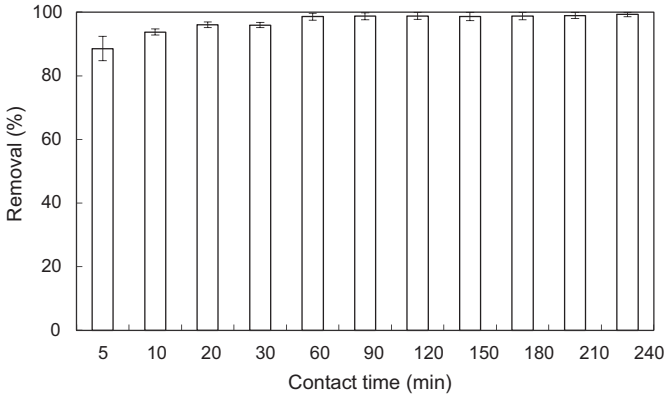

Fig. 11. Effect of contact time on the removal of RhB by surfactant- modified laterite (SML) (initial concentration Ci (RhB) = 10–5 M, pH 4, adsorbent mass 0.25 g, and 1 mM NaCl). Error bars show the standard deviations of three replicates.

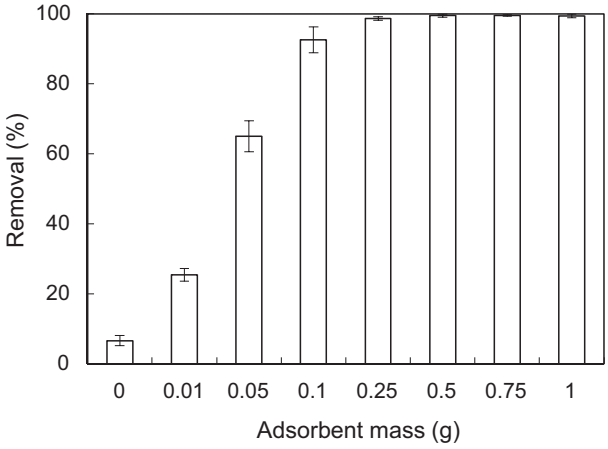

Fig. 12. Effect of pH on the removal of RhB by surfactant- modified laterite (SML) (initial concentration Ci (RhB) = 10–5 M, pH 4, contact time 60 min, 1 mM NaCl). Error bars show the standard deviations of three replicates.

Fig. 12 shows that the RhB removal of RhB increased dramatically when increasing the SML amount, reaching 99% with an adsorbent amount of 0.25 g. It was further observed that the RhB removal remained unchanged when the adsorbent dosage was higher than 0.25 g. Thus, it can be conducted that the optimum SML amount is 0.25 g, which was used for other studies.

3.3.4. Effect of ionic strength

The ionic strength plays a vital role in evaluating the influence of the electrostatic attraction between positive RhB ions and negatively charged SML surface. The desorption of SDS from the SML surface was also induced in the presence of salt. An ionic strength varying from 0 to 200 mM was applied to the solution containing 0.25 g SML with 10^{-5} M RhB and pH 4 to study the corresponding effect.

Fig. 13 indicates that the RhB removal decreased with an increase in NaCl concentration in the 0–200 mM range of. From 0 to 1 mM, the RhB removal only slightly decreased insignificantly while increasing dramatically at high ionic strength (100 and 200 mM NaCl). The decrease of the RhB removal by the reduction of electrostatic attraction [5] or the SDS desorption [9] upon increasing NaCl concentration was previously demonstrated.

To further evaluate the influence of the ionic strength, adsorption isotherms were examined as reported below.

3.3.5. Adsorption isotherms of RhB onto surfactant-modified laterite (SML)

The adsorption isotherms of RhB onto SML at three salt concentrations on the adsorption were investigated at pH 4 (Fig. 14).

Fig. 14 indicates that the capacity of RhB adsorption onto SML was reduced at all initial concentrations of RhB when the ionic strength increased in the 1–100 mM range. These results suggest that the RhB adsorption onto SML may be induced by the electrostatic attraction between the cationic RhB molecules and highly negatively charged SML. It should be noted that the Na^+ counter ions increased with increasing salt concentration, thus the RhB adsorption was screened by the competition between Na+ and cationic RhB [15]. As a result, the adsorption decreased with increasing NaCl concentrations. In addition, the adsorption isotherms of RhB onto SML were well represented by the two-step adsorption model, suggesting that the SDS desorption also occurred [9]. The adsorption reached a plateau when the initial concentration of RhB equaled 2×10^{-3} M. The maximum RhB adsorption capacity of 18 mg/g, which was observed at 1 mM NaCl, was decreased to 14.5 mg/g at 100 mM NaCl. All adsorption isotherms further demonstrated that the RhB adsorption onto SML is mainly controlled by the electrostatic attraction.

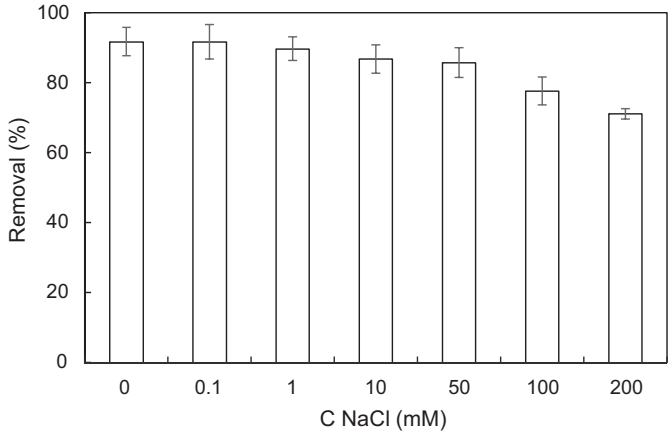

Fig. 13. Effect of pH on the removal of RhB by surfactant- modified laterite (SML) (initial concentration Ci (RhB) = 10–5 M, pH 4, contact time 60 min, adsorbent mass 0.25 g). Error bars show the standard deviations of three replicates.

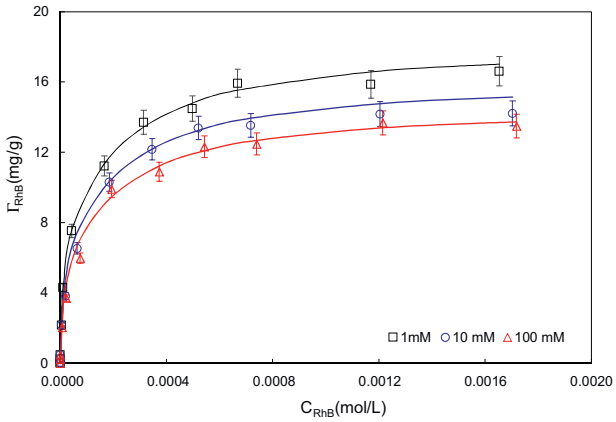

Fig. 14. Adsorption isotherms of RhB onto surfactant-modified laterite (SML) at three NaCl concentrations (pH 4). CRhB is the equilibrium RhB concentration. The experimental data are described by points while the solid lines are the results of 2-step adsorption model. Error bars show the standard deviations of three replicates.

3.3.6. Adsorption kinetics of RhB onto SML

The adsorption kinetics of RhB onto SML were carried out at the three initial RhB concentrations of 10^{-5}, 10^{-4} and 10^{-3} M from 0 to 240 min.

The following pseudo-second-order equation was used to predict the adsorption kinetic.

$$\frac{t}{q_t} = \frac{1}{k_k \cdot q_e^2} + \frac{1}{q_e} t \tag{6}$$

where q_e and q_t (mg/g) indicate adsorption capacities of RhB onto SML at equilibrium and time t, respectively, and k_k (g/mg·min) is the reaction rate constant of pseudo-second-order adsorption kinetics.

Fig. 15 shows that the pseudo-second order represented very well the experimental data for the three concentrations of RhB concentrations. The excellent value of R^2 (>0.994) demonstrated that the adsorption kinetics of RhB onto SML are in accordance with a pseudo-second-order model. Our results are similar to those obtained for the RhB adsorption onto kaolinite [50], in which pseudo-second-order was found to be the best model to describe the adsorption kinetics.

3.4. Comparison of the effectiveness of SML and other adsorbents for RhB removal

The laterite soil was modified by the SDS adsorption at low pH and ionic strength to revert the surface charge from weakly positive to

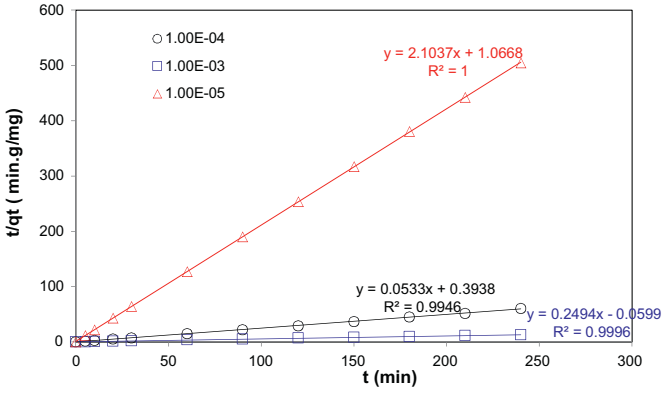

Fig. 15. The pseudo-second order for RhB adsorption onto surfactant-modified laterite (SML) with three initial concentrations.

highly negative. The removal of the cationic dye RhB significantly increased after the surface modification with SDS. Fig. 16 indicates the comparison between the removal of RhB using raw laterite without and with SDS modification. As it can be seen in Fig. 16, the RhB removal increased dramatically from 22.77 to 98.85% when using SML. To the best of our best knowledge, numerous scientific studies were conducted to investigate the RhB removal using different novel adsorbents. However, the removal of RhB using SML, which is systematically studied in this work, was not investigated so far. Table 4 shows that SML possesses the highest removal efficiency and adsorption capacity. This further demonstrates that SML is an eco-friendly and excellent adsorbent for the removal of RhB from aqueous solutions.

Although laterite is a natural soil and therefore inexpensive adsorbent, the reuse potential and stability of SML are desirable properties. The regeneration of SML by using NaOH and HCl was repeated five times. Fig. 17 shows the variation in RhB removal using SML after five cycles. A very small decrease in RhB removal is observed which remained nonetheless higher than 94.5% after five regenerations for both NaOH and HCl. The error bars show that the standard deviations after five cycles are also small, indicating that SML is a novel adsorbent that can be reused many times.

4. Conclusions

We have investigated the adsorption characteristics and mechanisms of SDS onto laterite soil with a positively and negatively charged surface at pH 4 and 10, respectively. XRF, TOC, SEM, BET, and zeta potential measurements were used to characterize the laterite soil before the adsorption study. At pH 4, the adsorption of SDS onto laterite was mainly controlled by the electrostatic attraction between anions and positively charged laterite surface. In contrast, the adsorption of SDS onto laterite surface at pH 10 was promoted by hydrophobic interactions between the alkyl chains of the surfactant and NOMs present in the laterite soil. The two-step adsorption model was successfully applied to fit the SDS adsorption isotherms onto laterite with differently charged surfaces at different NaCl concentrations. The use of SDS adsorption at low pH and ionic strength was explored to enhance the removal of the cationic dye RhB. Optimum parameters for RhB removal were an adsorption time of 60 min, pH 4, and adsorbent mass of 0.25 g. The removal efficiency of RhB reached 95% after five recycles while the maximum adsorption capacity of RhB was 18 mg/g. It can be concluded that the SDS adsorption onto laterite is needed to change the surface charge of laterite, and thus enhance the cationic dye removal from aqueous solutions.

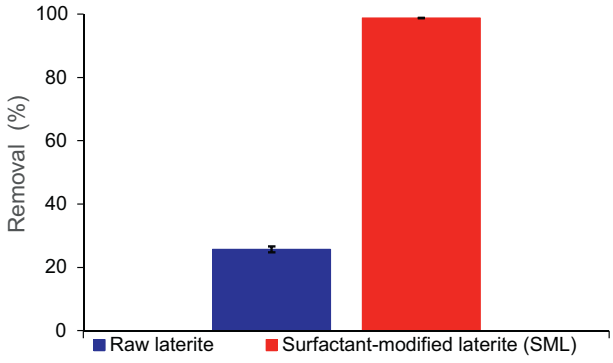

Fig. 16. Removal RhB using laterite soil with and without modification by SDS preadsorption (initial concentration Ci (RhB) = 10–5 M in 1 mM NaCl (pH 4)). Error bars show the standard deviations of three replicates.

Table 4
Adsorption capacity and removal efficiency of RhB using surfactant-modified laterite (SML) and other absorbents.

Adsorbent	Adsorption capacity (mg/g)	Removal efficiency (%)	References
Coir pith	2.56	79.4	[51]
Exhausted coffee ground	5.26	NI	[52]
Bentonite clay	7.7	91	[53]
Coal ash	2.86	NI	[54]
Surfactant-modified coconut coir pith	14.9	97	[15]
Surfactant-modified laterite (SML)	18.0	98.85	This study

NI: no information.

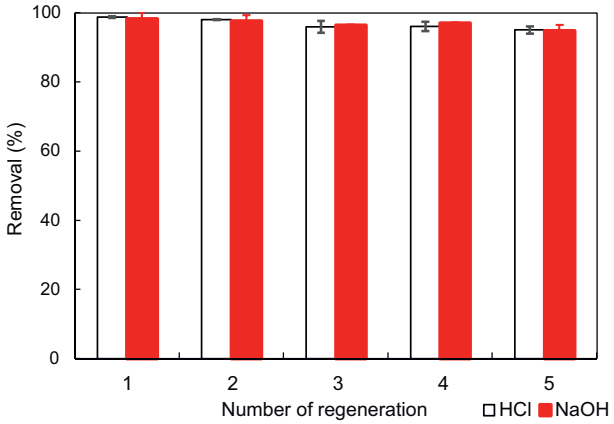

Fig. 17. Removal of RhB using SML after five regenerations. Error bars show standard deviation of three replicates.

CRediT authorship contribution statement

Tien Duc Pham: Conceptualization, Methodology, Validation, Investigation, Resources, Writing - original draft, Writing - review & editing, Visualization, Supervision, Project administration. **Thu Thao Pham:** Formal analysis, Data curation. **Minh Nguyet Phan:** Formal analysis, Data curation. **Thi Mai Viet Ngo:** Formal analysis. **Van Doan Dang:** Data curation. **Cuong Manh Vu:** Software, Validation, Writing - review & editing, Visualization.

Declaration of competing interest

The authors declare that they have no conflict of interest.

References

[1] J.R. Milton, T.K. Joy, Surfactants and Interfacial Phenomena, John Wiley&Sons, Inc, USA, 2012.
[2] Z. Adeel, R.G. Luthy, Sorption and transport kinetics of a nonionic surfactant through an aquifer sediment, Environ. Sci. Technol. 29 (1995) 1032–1042.
[3] S. Paria, Surfactant-enhanced remediation of organic contaminated soil and water, Adv. Colloid Interf. Sci. 138 (2008) 24–58.
[4] A. A., P. A., B. M., Removal of phenol from water environment by surfactant-modified alumina through adsolubilization, Colloids Surf. A Physicochem. Eng. Asp. 277 (2006) 63.
[5] T.P.M. Chu, N.T. Nguyen, T.L. Vu, T.H. Dao, L.C. Dinh, H.L. Nguyen, T.H. Hoang, T.S. Le, T.D. Pham, Synthesis, characterization, and modification of alumina nanoparticles for cationic dye removal, Materials 12 (2019) 450.
[6] M.U. Khobragade, A. Pal, Adsorptive removal of Mn(II) from water and wastewater by surfactant-modified alumina, Desalin. Water Treat. 57 (2016) 2775–2786.
[7] T.M.T. Nguyen, T.P.T. Do, T.S. Hoang, N.V. Nguyen, H.D. Pham, T.D. Nguyen, T.N.M. Pham, T.S. Le, T.D. Pham, Adsorption of anionic surfactants onto alumina: characteristics, mechanisms, and application for heavy metal removal, Int. J. Polym. Sci. 2018 (2018) 11.
[8] T.D. Pham, T.T. Do, V.L. Ha, T.H.Y. Doan, T.A.H. Nguyen, T.D. Mai, M. Kobayashi, Y. Adachi, Adsorptive removal of ammonium ion from aqueous solution using surfactant-modified alumina, Environ. Chem. 14 (2017) 327–337.
[9] T.D. Pham, T.T. Tran, V.A. Le, T.T. Pham, T.H. Dao, T.S. Le, Adsorption characteristics of molecular oxytetracycline onto alumina particles: the role of surface modification with an anionic surfactant, J. Mol. Liq. 287 (2019), 110900.

[10] M. Ishiguro, L.K. Koopal, Surfactant adsorption to soil components and soils, Adv. Colloid Interf. Sci. 231 (2016) 59–102.
[11] T.D. Pham, M. Kobayashi, Y. Adachi, Adsorption of anionic surfactant sodium dodecyl sulfate onto alpha alumina with small surface area, Colloid Polym. Sci. 293 (2015) 217–227.
[12] A. Adak, M. Bandyopadhyay, A. Pal, Removal of crystal violet dye from wastewater by surfactant-modified alumina, Sep. Purif. Technol. 44 (2005) 139–144.
[13] D.A. K., S. S., P. A., M.S. K., Surfactant-modified alumina: an efficient adsorbent for malachite green removal from water environment, J. Environ. Sci. Health A 44 (2009) 896.
[14] Y. Su, B. Zhao, W. Xiao, R. Han, Adsorption behavior of light green anionic dye using cationic surfactant-modified wheat straw in batch and column mode, Environ. Sci. Pollut. Res. 20 (2013) 5558–5568.
[15] M.V. Sureshkumar, C. Namasivayam, Adsorption behavior of Direct Red 12B and Rhodamine B from water onto surfactant-modified coconut coir pith, Colloids Surf. A Physicochem. Eng. Asp. 317 (2008) 277–283.
[16] Y.G. Mishael, P.L. Dubin, Uptake of organic pollutants by silica−polycation-immobilized micelles for groundwater remediation, Environ. Sci. Technol. 39 (2005) 8475–8480.
[17] Y.G. Mishael, T. Undabeytia, G. Rytwo, B. Papahadjopoulos-Sternberg, B. Rubin, S. Nir, Sulfometuron incorporation in cationic micelles adsorbed on montmorillonite, J. Agric. Food Chem. 50 (2002) 2856–2863.
[18] A. Radian, M. Carmeli, D. Zadaka-Amir, S. Nir, E. Wakshal, Y.G. Mishael, Enhanced removal of humic acid from water by micelle-montmorillonite composites: comparison to granulated activated carbon, Appl. Clay Sci. 54 (2011) 258–263.
[19] T.D. Pham, H.H. Nguyen, N.V. Nguyen, T.T. Vu, T.N.M. Pham, T.H.Y. Doan, M.H. Nguyen, T.M.V. Ngo, Adsorptive removal of copper by using surfactant modified laterite soil, J. Chem. 2017 (2017) 10.
[20] A. Maiti, J.K. Basu, S. De, Experimental and kinetic modeling of As(V) and As(III) adsorption on treated laterite using synthetic and contaminated groundwater: effects of phosphate, silicate and carbonate ions, Chem. Eng. J. 191 (2012) 1–12.
[21] J.K. Wolterink, L.K. Koopal, M.A.C. Stuart, W.H. Van Riemsdijk, Surface charge regulation upon polyelectrolyte adsorption, hematite, polystyrene sulfonate, surface charge regulation: theoretical calculations and hematite-poly(styrene sulfonate) system, Colloids Surf. A Physicochem. Eng. Asp. 291 (2006) 13–23.
[22] F. Al-Momani, E. Touraud, J.R. Degorce-Dumas, J. Roussy, O. Thomas, Biodegradability enhancement of textile dyes and textile wastewater by VUV photolysis, J. Photochem. Photobiol. A Chem. 153 (2002) 191–197.
[23] S.-F. Kang, C.-H. Liao, S.-T. Po, Decolorization of textile wastewater by photo-Fenton oxidation technology, Chemosphere 41 (2000) 1287–1294.
[24] N. Mohan, N. Balasubramanian, C.A. Basha, Electrochemical oxidation of textile wastewater and its reuse, J. Hazard. Mater. 147 (2007) 644–651.
[25] A.G. Vlyssides, M. Loizidou, P.K. Karlis, A.A. Zorpas, D. Papaioannou, Electrochemical oxidation of a textile dye wastewater using a Pt/Ti electrode, J. Hazard. Mater. 70 (1999) 41–52.
[26] S. Papić, N. Koprivanac, A. Lončarić Božić, A. Meteš, Removal of some reactive dyes from synthetic wastewater by combined Al(III) coagulation/carbon adsorption process, Dyes Pigments 62 (2004) 291–298.
[27] M.R. Almeida, R. Stephani, H. Dos Santos, L.F.C. Oliveira, Spectroscopic and theoretical study of the “azo”-dye E124 in condensate phase: evidence of a dominant hydrazo form, J. Phys. Chem. A 114 (2009) 526–534.
[28] M. Doğan, M. Alkan, A. Türkyilmaz, Y. Özdemir, Kinetics and mechanism of removal of methylene blue by adsorption onto perlite, J. Hazard. Mater. 109 (2004) 141–148.
[29] B.H. Hameed, M.I. El-Khaiary, Removal of basic dye from aqueous medium using a novel agricultural waste material: pumpkin seed hull, J. Hazard. Mater. 155 (2008) 601–609.
[30] T.D. Pham, M. Kobayashi, Y. Adachi, Adsorption characteristics of anionic azo dye onto large α-alumina beads, Colloid Polym. Sci. 293 (2015) 1877–1886.
[31] V.K. Gupta, P.J.M. Carrott, M.M.L. Ribeiro Carrott, Suhas, Low-cost adsorbents: growing approach to wastewater treatment—a review, Crit. Rev. Environ. Sci. Technol. 39 (2009) 783–842.
[32] V.K. Gupta, Suhas, Application of low-cost adsorbents for dye removal – a review, J. Environ. Manag. 90 (2009) 2313–2342.
[33] R. Atkin, V.S.J. Craig, E.J. Wanless, S. Biggs, Mechanism of cationic surfactant adsorption at the solid–aqueous interface, Adv. Colloid Interf. Sci. 103 (2003) 219–304.
[34] B.-Y. Zhu, T. Gu, Surfactant adsorption at solid-liquid interfaces, Adv. Colloid Interf. Sci. 37 (1991) 1–32.
[35] S. P., R. S., S. V., K.S. D., S. S., Removal of copper(II) ions from aqueous solution by adsorption using cashew nut shell, Desalination 266 (2011) 63.
[36] T.D. Pham, T.T. Bui, V.T. Nguyen, T.K.V. Bui, T.T. Tran, Q.C. Phan, T.D. Pham, T.H. Hoang, Adsorption of polyelectrolyte onto nanosilica synthesized from rice husk: characteristics, mechanisms, and application for antibiotic removal, Polymers 10 (2018) 220.
[37] T.D. Pham, T.T. Bui, T.T. Trang Truong, T.H. Hoang, T.S. Le, V.D. Duong, A. Yamaguchi, M. Kobayashi, Y. Adachi, Adsorption characteristics of beta-lactam cefixime onto nanosilica fabricated from rice HUSK with surface modification by polyelectrolyte, J. Mol. Liq. (2019) 111981.
[38] A.V. Delgado, F. González-Caballero, R.J. Hunter, L.K. Koopal, J. Lyklema, Measurement and interpretation of electrokinetic phenomena, J. Colloid Interface Sci. 309 (2007) 194–224.
[39] A. Maiti, H. Sharma, J.K. Basu, S. De, Modeling of arsenic adsorption kinetics of synthetic and contaminated groundwater on natural laterite, J. Hazard. Mater. 172 (2009) 928–934.
[40] A. Maiti, J.K. Basu, S. De, Development of a treated laterite for arsenic adsorption: effects of treatment parameters, Ind. Eng. Chem. Res. 49 (2010) 4873–4886.
[41] E.M. Lee, L.K. Koopal, Adsorption of cationic and anionic surfactants on metal oxide surfaces: surface charge adjustment and competition effects, J. Colloid Interface Sci. 177 (1996) 478–489.
[42] P. Somasundaran, J.T. Kunjappu, In-situ investigation of adsorbed surfactants and polymers on solids in solution, Colloids Surf. 37 (1989) 245–268.
[43] R. Zhang, P. Somasundaran, Advances in adsorption of surfactants and their mixtures at solid/solution interfaces, Adv. Colloid Interf. Sci. 123–126 (2006) 213–229.
[44] Y. Huang, A. Yamaguchi, T.D. Pham, M. Kobayashi, Charging and aggregation behavior of silica particles in the presence of lysozymes, Colloid Polym. Sci. 296 (2018) 145–155.
[45] T.D. Pham, T.U. Do, T.T. Pham, T.A.H. Nguyen, T.K.T. Nguyen, N.D. Vu, T.S. Le, C.M. Vu, M. Kobayashi, Adsorption of poly(styrenesulfonate) onto different-sized alumina particles: characteristics and mechanisms, Colloid Polym. Sci. 297 (2019) 13–22.
[46] M. Thongngam, D.J. McClements, Influence of pH, ionic strength, and temperature on self-association and interactions of sodium dodecyl sulfate in the absence and presence of chitosan, Langmuir 21 (2004) 79–86.
[47] L.K. Koopal, E.M. Lee, M.R. Böhmer, Adsorption of cationic and anionic surfactants on charged metal oxide surfaces, J. Colloid Interface Sci. 170 (1995) 85–97.
[48] S.-H. Song, P. Koelsch, T. Weidner, M.S. Wagner, D.G. Castner, Sodium dodecyl sulfate adsorption onto positively charged surfaces: monolayer formation with opposing headgroup orientations, Langmuir 29 (2013) 12710–12719.
[49] K. Kadirvelu, C. Karthika, N. Vennilamani, S. Pattabhi, Activated carbon from industrial solid waste as an adsorbent for the removal of Rhodamine-B from aqueous solution: kinetic and equilibrium studies, Chemosphere 60 (2005) 1009–1017.
[50] T.A. Khan, S. Dahiya, I. Ali, Use of kaolinite as adsorbent: equilibrium, dynamics and thermodynamic studies on the adsorption of Rhodamine B from aqueous solution, Appl. Clay Sci. 69 (2012) 58–66.
[51] C. Namasivayam, R. Radhika, S. Suba, Uptake of dyes by a promising locally available agricultural solid waste: coir pith, Waste Manag. 21 (2001) 381–387.
[52] K. Shen, M.A. Gondal, Removal of hazardous Rhodamine dye from water by adsorption onto exhausted coffee ground, J. Saudi Chem. Soc. 21 (2017) S120–S127.
[53] S.S. Tahir, N. Rauf, Removal of a cationic dye from aqueous solutions by adsorption onto bentonite clay, Chemosphere 63 (2006) 1842–1848.
[54] S. Wang, M. Soudi, L. Li, Z.H. Zhu, Coal ash conversion into effective adsorbents for removal of heavy metals and dyes from wastewater, J. Hazard. Mater. 133 (2006) 243–251.